

The drug loading impact on dissolution and diffusion: a case-study with amorphous solid dispersions of nevirapine

O impacto do carregamento de fármaco na dissolução e difusão: um estudo de caso com dispersões sólidas amorfas de nevirapina

El impacto de la carga farmacológica en la disolución y difusión: un estudio de caso con dispersiones sólidas amorfas de nevirapina

Received: 10/04/2022 | Revised: 10/17/2022 | Accepted: 10/18/2022 | Published: 10/23/2022

Kayque Almeida dos Santos

ORCID: <https://orcid.org/0000-0002-2576-1290>
Federal University of Pernambuco, Brazil
E-mail: kayque.almeida@ufpe.br

Lucas José de Alencar Danda

ORCID: <https://orcid.org/0000-0003-1526-1572>
Federal University of Pernambuco, Brazil
E-mail: lucasdanda@gmail.com

Thaísa Cardoso de Oliveira

ORCID: <https://orcid.org/0000-0002-4621-1626>
Federal University of Pernambuco, Brazil
E-mail: thaisa.cardoso@hotmail.com

José Lamartine Soares-Sobrinho

ORCID: <https://orcid.org/0000-0002-3280-0294>
Federal University of Pernambuco, Brazil
E-mail: joselamartine@hotmail.com

Monica Felts de La Roca Soares

ORCID: <https://orcid.org/0000-0002-4873-915X>
Federal University of Pernambuco, Brazil
E-mail: monica.soares@ufpe.br

Abstract

Amorphous solid dispersions (ASDs) are a viable alternative to enhance the kinetic solubility of poorly water-soluble drugs. However, there is lack of discussion about the impact of drug loading on dissolution rate and drug diffusion across the membrane generated by supersaturation. So, it was obtained amorphous solid dispersions with nevirapine and polyvinylpyrrolidone K-30 by solvent evaporation method using different drug loadings (10%, 15% and 20% w/w). Thermal analysis, Fourier transform infrared spectroscopy and x-ray diffraction characterized the ASDs, indicating that there was a good miscibility between components which stabilized the drug in its amorphous state. The intermolecular interactions impacted on the ASDs in vitro performance, where they were evaluated to dissolution tests under different conditions and permeability studies. All amorphous systems had an increment in aqueous solubility compared to nevirapine alone, although 10% amorphous solid dispersion (SD 10) kept drug supersaturation at very high concentrations longer, preventing the drug recrystallization, having the greater drug flux on membranes and more intermolecular interactions among the components. Therefore, large quantities of the polymer are required for the stability of the amorphous drug, due to the increase in the number of intermolecular interactions.

Keywords: Drug delivery system; Nevirapine; Dissolution; Permeability; Anti-retroviral agent.

Resumo

Dispersões sólidas amorfas (DSA) são uma alternativa viável para aumentar a solubilidade cinética de drogas mal solúveis em água. No entanto, há pouca discussão sobre o impacto do carregamento de drogas na taxa de dissolução e difusão de drogas em toda a membrana gerada pela supersaturação. Então, obteve-se dispersões sólidas amorfas com nevirapina e polivinilpirrolidona K-30 por método de evaporação de solvente utilizando diferentes cargas de drogas (10%, 15% e 20% p/p). Análise térmica, Espectroscopia de Infravermelho com Transformada de Fourier e Difração de Raios-X caracterizaram os DSA, indicando que houve uma boa compatibilidade entre os componentes, estabilizando a droga em seu estado amorfo. As interações intermoleculares impactaram no desempenho in vitro dos DSA, onde foram avaliadas para testes de dissolução em diferentes condições e estudos de permeabilidade. Todos os sistemas amorfos tiveram um incremento na solubilidade aquosa em comparação apenas com nevirapina, embora a dispersão sólida 10% (DS 10) manteve a supersaturação de drogas em concentrações muito altas por mais tempo,

impedindo a recristalização da droga, tendo o maior fluxo de drogas na membrana e mais interações intermoleculares entre os componentes. Portanto, grandes quantidades do polímero são necessárias para a estabilidade da droga amorfa, devido ao aumento do número de interações intermoleculares.

Palavras-chave: Sistema de liberação de medicamentos; Nevirapina; Dissolução; Permeabilidade; Antirretroviral.

Resumen

Las dispersiones amorfas sólidas (DSA) son una alternativa viable para aumentar la solubilidad cinética de los fármacos solubles en agua. Sin embargo, hay poca discusión sobre el impacto de la carga de fármacos en la tasa de disolución y difusión de fármacos a través de la membrana generada por la sobresaturación. Así que, las dispersiones sólidas amorfas con nevirapina y polivinilpirrolidona K-30 se obtuvieron por método de evaporación con disolvente utilizando diferentes cargas de fármaco (10%, 15% y 20% p/p). El análisis térmico, la espectroscopia infrarroja por transformada de Fourier y la difracción de rayos-X caracterizaron las DSAs, lo que indica que había una buena compatibilidad entre los componentes, estabilizando el fármaco en su estado de amorfo. Las interacciones intermoleculares impactaron la actuación *in vitro* de las DSA, donde fueron evaluados para pruebas de disolución bajo diferentes condiciones y estudios de permeabilidad. Todos los sistemas amorfos tuvieron un aumento de la solubilidad acuosa en comparación solo con la nevirapina, aunque la dispersión sólida al 10% (DS 10) mantuvo la sobresaturación del fármaco a concentraciones muy altas durante más tiempo, impidiendo la recristalización del fármaco, teniendo el mayor flujo de fármacos en la membrana y más interacciones intermoleculares entre los componentes. Por lo tanto, grandes cantidades del polímero son necesarias para la estabilidad del fármaco amorfo debido al creciente número de interacciones intermoleculares.

Palabras clave: Sistemas de liberación de medicamentos; Nevirapina; Disolución; Permeabilidad; Antirretrovirales.

1. Introduction

Nevirapine (NVP) is a non-nucleoside reverse transcriptase inhibitor analogue, widely used for antiretroviral pediatric treatment. However, NVP is a Class II drug in the biopharmaceutical classification system (BCS) (Sevam & Kulkarni, 2014), with a water solubility of $\sim 0.1 \text{ mg}\cdot\text{mL}^{-1}$ in neutral pH. As a poorly-soluble drug, it has a low dissolution rate and/or water solubility (0.1 mg/mL), which can compromise its oral bioavailability (Charalabidis et al., 2019; Kalepu & Nekkanti, 2015). To overcome this kind of limitation, drug release systems such as co-crystals (Caira et al., 2012), micelles (Moretton et al., 2014), nanosuspensions (Raju et al., 2014; Shegokar & Singh, 2011), nanoparticles (Kuo & Chung, 2011; Varshosaz et al., 2018) and amorphous solid dispersions (ASDs) (Datta et al., 2011; Lokamatha et al., 2011; Mamatha et al., 2017; Monschke & Wagner, 2019) were developed with several poorly-soluble drugs. However, ASD stands out for its simplicity of preparation and for generating high levels of drug concentrations (Pandi et al., 2020).

ASDs are defined as a dispersion of one or more drugs in an inert carrier, usually a water-soluble polymer, forming a single amorphous phase. ASDs have been used to increase the kinetic solubility or poorly-soluble drugs by keeping it dispersed in an amorphous state inside the polymer matrix and thus releasing it to form a supersaturated solution during non-sink dissolution (Djuris et al., 2013; Pandi et al., 2020; Tambosi et al., 2018). In amorphous state, drug molecules have an excess energy that lead to a greater transient solubility, when compared to their crystalline counterpart, which increases the dissolution rate (Figueirêdo et al., 2018; Schver & Lee, 2018). It is important that the ASD components have good miscibility to stabilize the solid dispersion and avoid phase separation and drug recrystallization in the solid state (Baghel et al., 2016). Such miscibility is favored by weak drug-polymer interactions, such as Van de Waals forces and hydrogen bonding (Shi et al., 2022).

Although the role of ASDs in increasing the kinetic solubility of poorly soluble drugs is widely discussed, there is still a lack of studies on drug diffusion and permeability through membranes, which is also an important step in absorption and bioavailability. Considering amorphous drugs generates a supersaturated solution, studying the permeation of dispersed systems becomes important to better understand the role of ASDs in the absorption of poorly-solubility drugs.

ASDs of NVP are not innovative, with studies focusing on increasing apparent solubility (Mamatha et al., 2017; Monschke & Wagner, 2019), but there is insufficient discussions on how drug loading impacts drug supersaturation or drug

permeability. Considering the importance of supersaturation generated by ASDs, this study aimed to develop ASDs based on NVP and PVP with different drug loadings in laboratory by the solvent evaporation technique to assess their impacts on drug permeability caused by different supersaturated amorphous systems.

2. Methodology

Nevirapine was chosen to be a drug model, mainly because is a BCS class II and it's used as a pediatric antiretroviral to children and mother to combat HIV infection. Accordingly, this study used it to better understand the effects of drug loadings on ASD through a quantitative case-study using physico-chemical techniques to achieve our goal.

2.1 Materials

Nevirapine was acquired from Farmanguinhos (Rio de Janeiro, Brazil). Polyvinylpyrrolidone (PVP, K30 grade) was donated by IMEC® (Custódia, Brazil). A semipermeable regenerated cellulose dialysis membrane was purchased from Spectrum Laboratories Inc. (California, United States) with a molecular mass limit of 14 kDa. All reagents, salts and solutions were obtained commercially with reagent grade and used as received.

2.2 Preparation of ASDs

ASDs containing NVP and PVP were prepared by solvent evaporation method since it is a simple and easily obtainable technique for the amorphous systems (Bhujbal et al., 2021). This procedure was carried out as Danda et al., 2019; Figueirêdo et al., 2018. A precise amount of NVP and PVP was simultaneously dissolved in ethanol at a 10:90, 15:85 or 20:80 proportion (NVP:PVP) to prepare for 10, 15 and 20% (wt/wt%) drug loading ASDs. The drug:polymer ethanol solution was put in an ultrasound bath for 30 min to ensure complete dissolution. Solutions were poured on 9 cm diameter non-adherent silicone cylindrical dishes and dried at a conventional lab oven at 60 °C. Films were removed from the dishes after 3 hours and returned to the oven for residual solvent removal for an additional 24 h. The resulting films were crushed in a porcelain mortar with the aid of liquid nitrogen and powders were passed through a 150 µm sieve. Final ASD powders were named after their NVP content (SD10, SD15 and SD20 for 10, 15 and 20% drug loadings) and stored in desiccators.

2.3 Solid state characterizations

The differential scanning calorimetry (DSC) curves were obtained on a Shimadzu® scanning calorimeter, model DSC-50, interconnected with the Shimadzu® TA-60WS software attached with a pure nitrogen gas cylinder at a flow rate of 50 mL.min⁻¹ in the temperature range 30–300 °C. Samples were placed in hermetically sealed aluminum specimen holders with a mass of 2 mg (± 0.1 mg) of sample. 99.9% pure metal indium was used to calibrate the temperature scale and enthalpy response.

X-ray diffraction analyzes were performed on a Siemens X-Ray Diffractometer D-500 diffractometer equipped with a copper anode. The 2θ angle range was between 5-40° with a digitizing speed of 0.02° 2θ/s, prepared on glass supports with a thin layer of powder material without solvent.

Fourier transform infrared spectra in the middle region were obtained using a PerkinElmer® equipment (model 400) equipped with attenuated total reflection (ATR) device with zinc selenide crystal. Samples were transferred directly to the ATR device compartment, with the aid of a spatula, having a "blank" analysis performed and cell-cleaning with acetone between each assay. The result was obtained in transmittance mode by averaging 16 spectrum scans, obtained from 4000–650 cm⁻¹ at 4 cm⁻¹ resolutions.

2.4 Crystalline NVP equilibrium solubility

The equilibrium solubility (C_s) of crystalline NVP was determined in pH 1.2 (potassium chloride + hydrochloric acid) and 6.8 buffer (monobasic potassium phosphate + sodium hydroxide), prepared according to USP 38. Erlenmeyer flasks containing 10 mL of buffer were saturated with excess crystalline NVP and kept at 37 °C under agitation at 150 rpm on an orbital shaker (Ethik Technology, São Paulo, Brazil) for 2 days. Samples were centrifuged at 12000 rpm for 5 minutes and an aliquot was removed and diluted with the buffer for quantitation on a Varian Cary 50 UV-Vis spectrophotometer (Agilent Technologies, California, United States). Absorbances were collected at 281 nm and compared to a NVP calibration curve prepared in the range of 2-30 $\mu\text{g}\cdot\text{mL}^{-1}$.

2.5 Dissolution Studies

To evaluate the dissolution rate and kinetic solubility profile of NVP released from ASDs and crystalline NVP, dissolution studies were conducted under sink and non-sink conditions. As NVP is a weak base ($\text{pK}_a = 2.8$) and demonstrates a high solubility in acidic medium (3 $\text{mg}\cdot\text{mL}^{-1}$) (S. Li et al., 2017), pH 6.8 buffer was chose as dissolution medium.

For the sink dissolution study, an amount equivalent to 20 mg NVP was introduced to a vessel filled with 250 mL dissolution medium constantly maintained at 37 ± 0.5 °C in a VanKel VK-7010 dissolution system (Agilent Technologies, California, United States) equipped with a USP 2 paddle apparatus at 75 rpm. At each predetermined time, 1 mL samples were collected and centrifuged at 12000 rpm for 5 minutes. An aliquot of the centrifuged sample was carefully diluted with dissolution medium for spectrophotometric quantitation as described previously. Experiments were run in triplicate. To investigate the differences among each ASD and compare it to crystalline NVP performance under sink conditions, the dissolution efficiency (DE%) was calculated based on the area under the curve (AUC) achieved by each system within the dissolution time interval (Eq. 1):

$$\text{DE}\% = \frac{\text{AUC}}{\text{Total rectangle area}} \times 100 \quad (\text{Equation 1})$$

where *total rectangle area* refers to the maximum AUC achievable, obtained by multiplying the X and Y values from the dissolution graph. Besides, the t_{max} indicates the time when the maximum concentration (C_{Max}) occurs and was also evaluated to compare the differences between the systems submitted to the test.

The kinetic solubility profiles of NVP released from ASDs was evaluated by a non-sink dissolution study, which was conducted using an Erweka DT-60 dissolution system (Erweka, Heusenstamm, DE) equipment with an adapted reduced-volume paddle & vessel set (Danda et al., 2019). To promote supersaturating dissolution conditions, an amount of each ASD equivalent to 25 mg NVP was introduced to 25 mL dissolution medium constantly maintained at 37 ± 0.5 °C and 150 rpm. This translated to a final NVP theoretical maximum concentration of 1000 $\mu\text{g}\cdot\text{mL}^{-1}$, which is approximately 10 times the NVP C_s in pH 6.8 (101.26 $\mu\text{g}\cdot\text{mL}^{-1}$, experimentally determined). Aliquots were collected at predetermined time (5, 10, 15, 20, 30, 45, 60, 90, 120, 240 min). Sample processing & quantitation was conducted the same way as previously. Experiments were run in triplicate.

2.6 Permeability studies

An in vitro permeability study was conducted according to an adapted version of Lakshman et al. (2020) with Franz-type diffusion cells to assess the influence of supersaturation in the passage of molecules of NVP across the membrane. Non-

sink conditions were necessary to maintain the supersaturation of the medium where the ASDs were submitted.

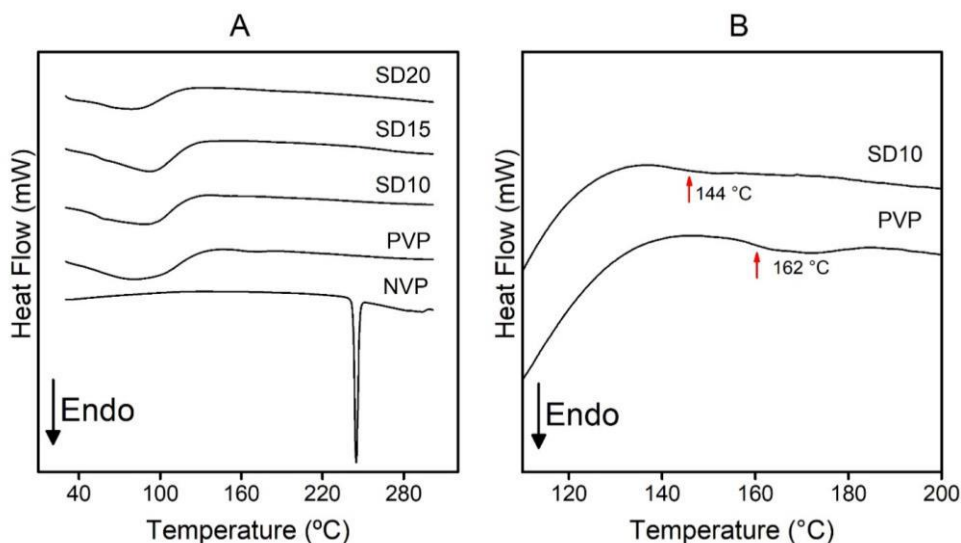
Initially, ASD solutions were prepared according to their respective NVP C_{max} achieved in the non-sink dissolution study. A crystalline NVP solution was also prepared at NVP C_s in pH 6.8. Immediately after preparation, 3 mL of either solution were placed onto semipermeable cellulose dialysis membranes (Spectrum Laboratories, Inc., CA, USA) attached to the Franz-type cell apparatus. Membranes had a molecular mass limit of 14 kDa and 1.77 cm² surface area. The recipient compartment was filled with 6.5 mL of Hanks Balanced Salt Solution (NaCl 0.14 M, KCl 0.005 M, CaCl₂ 0.001 M, MgSO₄ · 7H₂O 0.0004 M, MgCl₂ · 6H₂O 0.0005 M, NaHPO₄ · 2H₂O 0.0003 M, KH₂PO₄ 0.004 M, D-Glucose 0.006 M, NaHCO₃ 0.004 M) and kept under constant agitation, chosen to maintain the biorelevance of diffusion experiments. Samples were collected from the receptor compartment at predetermined time intervals (5, 10, 15, 20, 30, 45, 60, 90, 120, 180 and 240 minutes) and analyzed by spectrophotometry as described previously. Experiments were run in triplicate.

3. Results and Discussion

3.1 Solid state characterizations

Solid state characterizations comprise a set of techniques used to better understand the crystalline matter aspect of the obtained system.

Figure 1 - DSC curves of NVP, PVP and ASDs (A) and approximate curves of SD10 and PVP for T_g observation (B).



Source: Authors (2022).

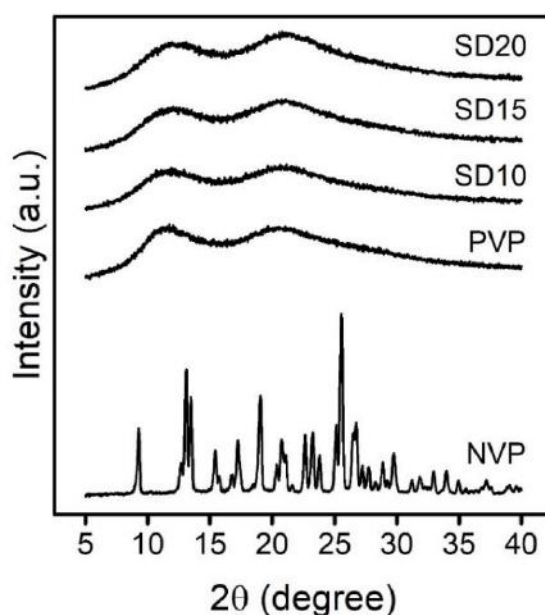
Figure 1A shows the DSC curves patterns of NVP, PVP and ASDs, where the endothermic peaks indicates the crystalline nature of the drug. So, the NVP curve points to an endothermic peak at 244 °C which corresponds to the melting peak with a band starting at 240 °C (Ahire et al., 2010). In the PVP curve, there is a broad region with an endothermic peak at 81 °C that refers to the dehydration process. Since PVP is a very hygroscopic polymer (Wypych, 2012), it tends to absorb moisture from the environment.

At 162 °C, the baseline shift is due to a change in polymer heat capacity (Figure 1B), indicating the polymer glass transition (T_g). The ASDs curves did not present any characteristic melting peak of the drug, suggesting that the drug is either molecularly dispersed in its amorphous state or dissolved in the polymer. In SD 10%, a baseline change was found at 144 °C in

Figure 2B, which shows the T_g of this system. This temperature was shifted to the left compared to pure PVP curve, showing a possible drug-polymer interaction.

T_g is a property of amorphous materials and is used to indicate their physical stability, especially regarding molecular mobility that changes above and below T_g (Alhalaweh et al., 2015). When two materials with different T_g are mixed together, the final T_g of the mixture usually finds itself between the T_g of the two components (Penzel et al., 1997; Saboo et al., 2020a). The T_g event was not observed in the other systems, due the variation in drug concentration. As the drug loading decreases, further the system T_g will be in relation to that of the polymer (Saboo et al., 2020b). Therefore, the higher drug loading systems had a lower T_g , with the baseline deviation more to left, which may have been overlapped by the polymer dehydration range.

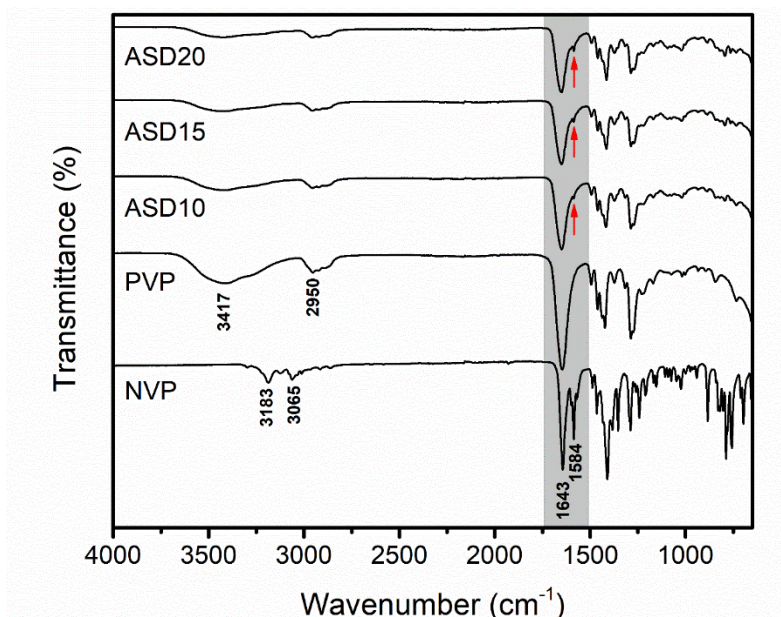
Figure 2 - XRPD patterns of NVP, PVP and ASDs.



Source: Authors (2022).

PXRD patterns are illustrated in Figure 2. NVP crystallizes into a monocyclic centrosymmetric structure, with four molecules per cell unit, but with an independent molecule with four multiplicities, adopting a butterfly conformation, as Mui et al. (1992) determined. It presents a set of distinct peaks (e.g., at 9.28, 13.08, 13.48, 19.02 and 25.54° 2θ) that characterizes its crystalline form (Chadha et al., 2010). On the other hand, as an amorphous polymer, PVP does not show diffraction planes and, consequently, an absence of apparent peaks is observed. As for the ASDs, no characteristic peaks of the NVP crystalline structure were observed, confirming that the drug is either dissolved or dispersed in the amorphous form with PVP, with no difference being observed between the three systems. The similarity between the diffraction spectra of the ASDs suggests that the drug-polymer interactions were enough to prevent drug recrystallization up to the 20% drug loading.

Figure 3 - Fourier Transform Infrared spectrums of NVP, PVP and ASDs between 4000-650 cm^{-1} .



Source: Authors (2022).

The infrared absorption spectra of the drug, polymer and ASDs are presented in Figure 3. NVP structure is characterized by an amide function in a seven-membered ring that adopts a planar conformation, also having a cyclopropyl substituent (Ayala et al., 2007a; Mui et al., 1992b). These groups are represented in the NVP spectrum by the bands at 3183 and 1643 cm^{-1} , which correspond to the vibrational nodes of the N-H and C=O stretch, respectively, of the amide group. The spectrum also shows bands at 3119 cm^{-1} corresponding to the C-H bond of the cyclopropyl substituent and at 1584 cm^{-1} that characterizes the scissors vibrations of the methyl group.

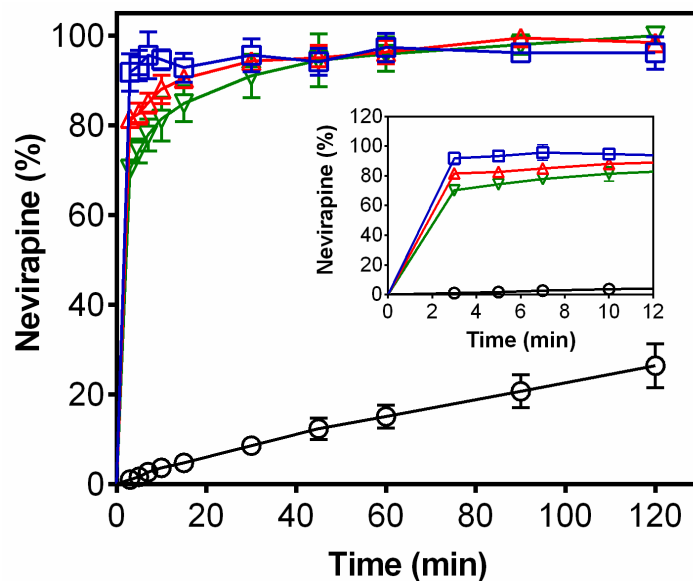
The PVP spectrum shows a band at 3417 cm^{-1} due to the O-H bond. This signal occurs due to the hygroscopicity of the polymer from moisture, also indicated from DSC results. It also shows a characteristic C-H stretch bands at 2950 cm^{-1} and 2879 cm^{-1} and C=O at 1465 cm^{-1} . ASDs indicated a change of bands in the three systems. The NVP N-H stretch band at 3183 cm^{-1} is not shown in the system spectra and there is a shift and widening of the C=O stretch band at 1643 cm^{-1} to the left and a decrease in signal strength. The characteristic band of NVP methyl group scissor vibrations in dispersions represented by red arrows have low intensity, but they grow as the drug loading increases.

Band shifts and band resource omissions usually suggests interaction between drug and polymer, as commonly occurs via hydrogen bonding in ASDs (Shi, et al., 2022), an important feature to avoid the process of recrystallization (Saboo et al., 2020a). NVP has an amide group that can interact with PVP's carbonyl group by hydrogen bonding, which explains changes in the peaks of the spectrum bands in the systems. Another possible interaction site between the components is with the NVP methyl pyridine with PVP carbonyl groups, which explains the intensity reduction of the characteristic band of this portion of the drug. This group is important for maintaining the crystal structure of the drug, being one of the portions responsible for the bonds between the drug molecules to form the crystal lattice (Ayala et al., 2007b). It is noted that as the drug concentration is increased, the characteristic peak of this group becomes more evident, suggesting that the miscibility between the two components decreases proportionally to the increase of the drug concentration.

3.2 Dissolution studies

Dissolution results under sink conditions are represented in Figure 4. Crystalline NVP was unable to reach 100% release at the end of the experiment, unlike ASDs that reached total release in less than 60 min. All ASDs were able to increase the dissolution rate of NVP, with a high drug release rate compared to its crystalline form.

Figure 4 - Dissolution profiles under sink conditions at pH 6.8 of SD10 (□), SD15 (△), SD20 (▽) and crystalline NVP (○). Error bars represent standard deviation (n = 3).



Source: Authors (2022).

The capacity of ASDs to increase the apparent aqueous solubility of poorly soluble drugs is well-known (Janssens & Van den Mooter, 2009; Zhang et al., 2018), which is one of the main advantages of amorphous formulations (Guan et al., 2019; Indulkar et al., 2019; Krstić et al., 2020). In brief, for a crystalline drug to interact with a solvent and dissolve in it, the interactions between the molecules in the crystal lattice must be disrupted for drug molecules to break free of the crystal structure. On the other hand, amorphous materials have no crystalline lattice interactions or bonds that need to be broken for the drug to interact with the solvent molecules and thus dissolve.

Several steps are reported to influence the release rate of an incorporated drug in ASDs, such as the transport of the dissolution medium to the polymer matrix, the swelling of the gel-forming polymer, the diffusion of the drug through the swollen polymer layer and the erosion of the swollen polymer (Ranga Rao & Devi, 1988). PVP is a hydrophilic polymer with faster erosion compared to other water-soluble polymers, which can explain the rapid release of NVP upon polymer dissolution (Grohganz et al., 2014; Lopes et al., 2005; Meenakshi & Khan, 2017; Punčochová et al., 2016).

However, it is observed that the lower the drug loading in the solid dispersion, the faster it was released from the polymer matrix (Table 1), with slight differences at the beginning of the dissolution assay. As such, the main difference between the tested drug loading levels was shown to be the t_{max} at which 100% drug release was achieved, which gradually increased with the NVP content in ASDs (SD10 > SD15 > SD20). The possible intermolecular interactions between the drug and the polymer may be responsible, since the higher the drug loading, the less intense were the interactions between them. The more drug there is in the system, the more likely there are drug-drug interactions and less drug-polymer interactions, which may compromise the dissolution performance of an ASD due to lesser amorphous drug. However, all NVP-PVP ASDs

in this work demonstrated rapid dissolution profile with a substantial increase in dissolution rate compared to pure crystalline NVP, which resulted in high DEs(%) (Table 1), which respect to the theoretical highest possible AUC achievable (12000 $\% \cdot \text{min}^{-1}$).

Table 1 - Dissolution parameters from sink dissolution tests with crystalline nevirapine and its amorphous solid dispersions with PVP at 10, 15 and 20% drug loading.

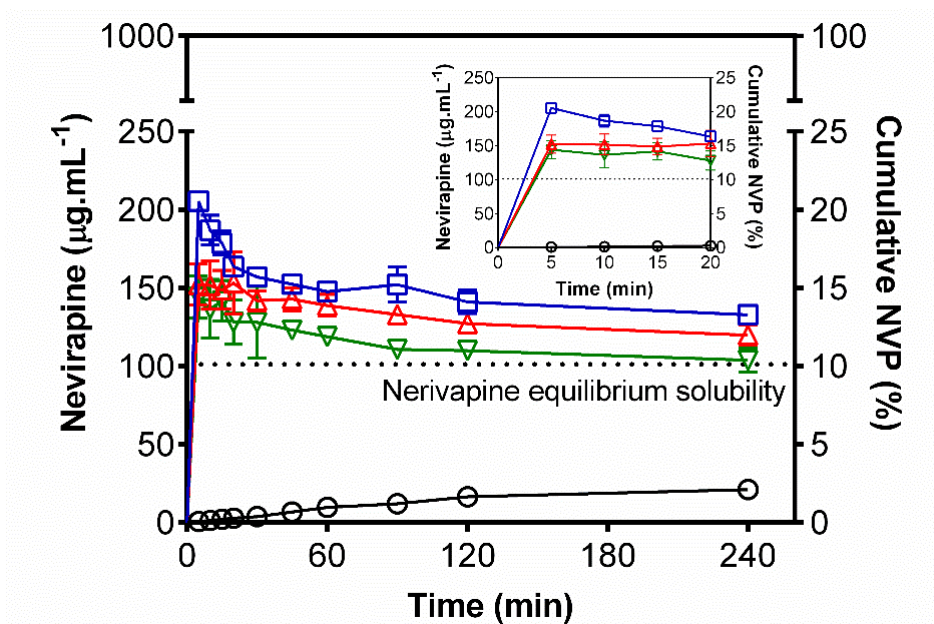
	Crystalline NVP	SD10	SD15	SD20
t_{\max} (min)	120	60	90	120
AUC ($\% \cdot \text{min}^{-1}$) ¹	1744 ± 302	11193 ± 232	11189 ± 149	10972 ± 368
DE% ^{1,2}	14.53 ± 2.51	93.28 ± 1.94	93.25 ± 1.24	91.43 ± 3.07

¹ Results of AUC and DE% from SD10, SD15 and SD20 were statistically equal between groups ($p > 0.05$).

² DE%: dissolution efficiency, calculated according to Eq. 1, assuming a total rectangle AUC of 12000 $\% \cdot \text{min}^{-1}$.
 Source: Authors (2022).

Dissolution studies under non-sink conditions were carried out to analyze the ability of dispersed NVP systems to generate drug supersaturation, as well as its recrystallization profile. Results are shown in Figure 5. All ASDs were able to exceed the crystalline NVP equilibrium solubility (101.65 $\mu\text{g} \cdot \text{mL}^{-1}$), reaching a supersaturation and maximum peak concentrations (C_{\max}) of 144.04, 153.01 and 205.45 $\mu\text{g}/\text{mL}$ (SD20, SD15 and SD10, respectively) before an ongoing drop in NVP concentration due to nucleation and recrystallization. On the other hand, crystalline NVP reached only 21.13 $\mu\text{g} \cdot \text{mL}^{-1}$ and was unable to reach its equilibrium before dissolution had terminated (4h). Since both crystalline NVP and ASDs had all the same average particle size, this is most possibly associated with a low dissolution rate of NVP crystals.

Figure 5 - Dissolution of NVP under non-sink condition at pH 6.8 released from SD10 (\square), SD15 (\triangle), SD20 (∇) and crystalline NVP (\circ). The dotted line represents the experimentally-determined crystalline NVP C_s (101.26 $\mu\text{g} \cdot \text{mL}^{-1}$). Error bars represent standard deviation ($n = 3$).



Source: Authors (2022).

ASDs based on hydrophilic polymers such as PVP usually demonstrate kinetic solubility profiles in which the higher the supersaturation achieved, the faster the drop in drug concentration generated by the consequent nucleation and recrystallization (Sun & Lee, 2015a, 2015c). In this scenario, C_{\max} can usually be considered as a critical factor where drug concentration may exceed the metastable zone upon which spontaneous nucleation and recrystallization occurs at a faster rate (Sun & Lee, 2013, 2015b). In this sense, SD10 released NVP slightly faster and reached a higher concentration, which seems to have also triggered a faster recrystallization, while SD15 and SD20 managed to maintain their supersaturation levels longer despite having also recrystallized. The reverse effect of drug loading on supersaturation sustenance is because dissolution is mainly controlled by the major component in the ASD system (i.e., the polymer in this case). As the amount of polymer decreases, dissolution tends to be increasingly controlled by the poorly soluble drug (Craig, 2002; Figueirêdo et al., 2018).

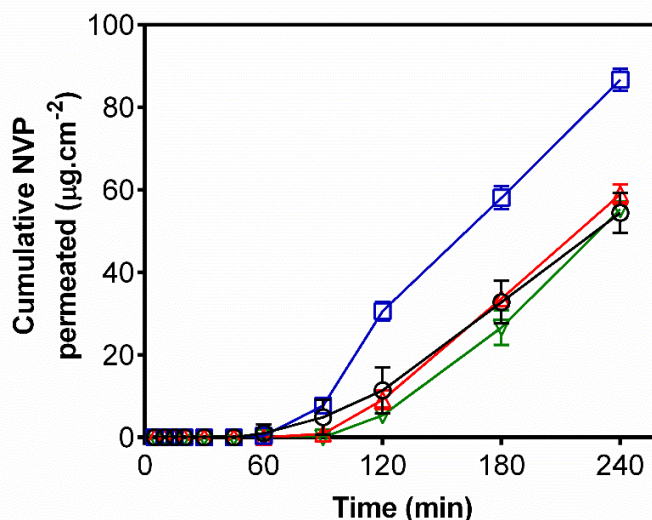
The drop in concentration is quite rapid before a complete drug release can be achieved in the non-sink dissolution conditions and is also influenced by the accelerated speed of recrystallization that the NVP has (N. Li et al., 2016). Despite this fact, SD10 was able to maintain NVP concentration at a slightly higher level, with a more sustained supersaturation, when compared to SD15 and SD20.

3.3 Permeability study

The impact of the differences generated by the drug loading effect were further investigated in a diffusion study, conducted under supersaturated conditions generated by the non-sink dissolution to reflect the true kinetic solubility profile of ASD systems. Considering that the absorption occurs once the drug is already dissolved and that the NVP releases from the ASDs were immediate, the diffusion studies occurred in sequence to such dissolution. Therefore, crystalline NVP and ASDs solutions were prepared according to their respective C_{\max} obtained by each system and were immediately submitted to the diffusion apparatus so that the diffusion study would occur in a continuous manner to the dissolution, enabling the evaluation of the impact of supersaturation and recrystallization on NVP diffusion.

The diffusion profiles of crystalline NVP and ASDs are shown in Figure 6. SD10 reached an amount of $86.73 \pm 2.66 \mu\text{g}/\text{cm}^2$, while SD15 and SD20 had profiles similar to crystalline NVP, with 58.93 ± 2.34 , 55.30 ± 1.63 and $54.46 \pm 4.82 \mu\text{g}/\text{cm}^2$, respectively. The permeated amount of NVP from SD10 was 1.6 times higher than that of crystalline NVP.

Figure 6 - NVP mass accumulated in Franz-type diffusion cells after release from SD10 (\square), SD15 (\triangle), SD20 (∇) and crystalline NVP (\circ). Diffusion occurred through a cellulose membrane. Error bars represent the standard deviation ($n = 3$).



Source: Authors (2022).

Among other influencing factors, the amount of permeation is dependent on the degree of molecular dispersion of the drug in the donor medium (Trasi & Taylor, 2015). Because the drug is in a more soluble/dispersed amorphous form inside an ASD, it disperses more widely in the medium while generating supersaturation. This leads to a huge difference in the gradient between the two compartments, which promotes greater permeation as the donor compartment is more drug-concentrated (Frank et al., 2012; Lakshman et al., 2020b). For having generated a greater supersaturation in relation to the others, SD10 had a greater driving force with more drug permeating the membrane, since the diffusion process occurs passively. However, although SD15 and SD20 generated supersaturation during the non-sink dissolution, they demonstrated permeation profiles similar to that of crystalline NVP. This might be associated to the drop in concentration caused by recrystallization, in addition to lower C_{max} when compared to SD10.

Additionally, SD10 may have formed a colloidal system through liquid-liquid phase separation (LLPS), which commonly occurs in supersaturated solutions above the amorphous equilibrium solubility, usually with low drug loading ASDs (Hate et al., 2019; Ilevbare & Taylor, 2013). Under LLPS, it is reported the formation of a drug domain with amorphous drug-rich nanodroplets that act as a reservoir, releasing amorphous drug into the water phase until it is depleted (Indulkar et al., 2016; Raina et al., 2014). With supersaturation being maintained by such events, the drug flux through the membrane can be higher due to the high concentration gradient. Thus, the amount of polymer in an ASD can deeply influence the drug diffusion upon release from the dissolved carrier.

4. Conclusion

This study showed that amorphous solid dispersions are a good strategy to improve the dissolution of nevirapine and to maintain the amorphous state. The intermolecular interaction between drug and polymer were the most important factor for the performance of solid dispersions, which may explain the main differences between the three drug loadings generated. The SD10 was the system who had the best in-vitro performance, having more polymer available to stabilize the amorphous drug and more drug-polymer interactions being formed. The ASDs systems obtained in this work were able to present a new presentation for NVP, in its amorphous state with improved dissolution and high permeation rate that can open new perspectives for HIV treatment. However, it is important to understand that amorphous solid dispersions with two or more drugs is desirable for polydrug therapies, such as antiretroviral. So, more studies are necessary to develop and characterize systems with two or more drugs to better care for HIV-positive patients.

Acknowledgments

The authors would like to thank Coordination of Improvement of Higher Education Personnel (CAPES) for research funding, Northeast Strategic Technologies Center (CETENE) and Drug Technology Laboratory (LTM) of the Federal University of Pernambuco for solid state characterizations.

References

- Ahire, B. R., Rane, B. R., Bakliwal, S. R., Pawar, S. P., College, P. S. G. V. P. M., & Nandurbar, D. (2010). Solubility Enhancement of Poorly Water Soluble Drug by Solid Dispersion Techniques. *International Journal of PharmTech Research*, 2(3), 2007–2015.
- Alhalaweh, A., Alzghoul, A., Mahlin, D., & Bergström, C. A. S. (2015). Physical stability of drugs after storage above and below the glass transition temperature: Relationship to glass-forming ability. *International Journal of Pharmaceutics*, 495(1), 312–317. <https://doi.org/10.1016/j.ijpharm.2015.08.101>
- Ayala, A. P., Siesler, H. W., Wardell, S. M. S. V., Boechat, N., Dabbene, V., & Cuffini, S. L. (2007a). Vibrational spectra and quantum mechanical calculations of antiretroviral drugs: Nevirapine. *Journal of Molecular Structure*, 828(1–3), 201–210. <https://doi.org/10.1016/j.molstruc.2006.05.055>
- Ayala, A. P., Siesler, H. W., Wardell, S. M. S. V., Boechat, N., Dabbene, V., & Cuffini, S. L. (2007b). Vibrational spectra and quantum mechanical calculations of antiretroviral drugs: Nevirapine. *Journal of Molecular Structure*, 828(1–3), 201–210. <https://doi.org/10.1016/j.molstruc.2006.05.055>

- Baghel, S., Cathcart, H., & O'Reilly, N. J. (2016). Theoretical and experimental investigation of drug-polymer interaction and miscibility and its impact on drug supersaturation in aqueous medium. *European Journal of Pharmaceutics and Biopharmaceutics*, *107*, 16–31. <https://doi.org/10.1016/j.ejpb.2016.06.024>
- Bhujbal, S. v., Mitra, B., Jain, U., Gong, Y., Agrawal, A., Karki, S., Taylor, L. S., Kumar, S., & (Tony) Zhou, Q. (2021). Pharmaceutical amorphous solid dispersion: A review of manufacturing strategies. *Acta Pharmaceutica Sinica B*, *11*(8), 2505–2536. <https://doi.org/10.1016/j.apsb.2021.05.014>
- Caira, M. R., Bourne, S. A., Samsodien, H., Engel, E., Liebenberg, W., Stieger, N., & Aucamp, M. (2012). Co-crystals of the antiretroviral nevirapine: Crystal structures, thermal analysis and dissolution behaviour. *CrystEngComm*, *14*(7), 2541–2551. <https://doi.org/10.1039/c2ce06507j>
- Chadha, R., Arora, P., Saini, A., & Jain, D. S. (2010). Solvated Crystalline Forms of Nevirapine: Thermoanalytical and Spectroscopic Studies. *AAPS PharmSciTech*, *11*(3), 1328–1339. <https://doi.org/10.1208/s12249-010-9511-z>
- Charalabidis, A., Sfouni, M., Bergström, C., & Macheras, Panos. (2019). The Biopharmaceutics Classification System (BCS) and the Biopharmaceutics Drug Disposition Classification System (BDDCS): Beyond guidelines. *International Journal of Pharmaceutics*, *566*, 264–281. <https://doi.org/10.1016/j.ijpharm.2019.05.041>
- Craig, D. Q. M. (2002). The mechanisms of drug release from solid dispersions in water-soluble polymers. In *International Journal of Pharmaceutics* (Vol. 231, Issue 2, pp. 131–144). Elsevier. [https://doi.org/10.1016/S0378-5173\(01\)00891-2](https://doi.org/10.1016/S0378-5173(01)00891-2)
- Danda, L. J. de A., Batista, L. de M., Melo, V. C. S., Soares Sobrinho, J. L., & Soares, M. F. de L. R. (2019). Combining amorphous solid dispersions for improved kinetic solubility of posaconazole simultaneously released from soluble PVP/VA64 and an insoluble ammonio methacrylate copolymer. *European Journal of Pharmaceutical Sciences*, *133*, 79–85. <https://doi.org/10.1016/j.ejps.2019.03.012>
- Datta, A., Ghosh, N. S., Gosh, S., Samanta, T., & Das, R. C. (2011). Enhancement of Solubility and Dissolution Profile of Nevirapine By Solid Dispersion Technique. *International Journal of Chemistry Research*, *2*(3), 53–58.
- Djuric, J., Nikolakakis, I., Ibric, S., Djuric, Z., & Kachrimanis, K. (2013). Preparation of carbamazepine-Soluplus® solid dispersions by hot-melt extrusion, and prediction of drug-polymer miscibility by thermodynamic model fitting. *European Journal of Pharmaceutics and Biopharmaceutics*, *84*(1), 228–237. <https://doi.org/10.1016/j.ejpb.2012.12.018>
- Figueirêdo, C. B. M., Nadvorny, D., Vieira, A. C. Q. de M., Schver, G. C. R. de M., Soares Sobrinho, J. L., Rolim Neto, P. J., Lee, P. I., & Soares, M. F. de L. R. (2018). Enhanced delivery of fixed-dose combination of synergistic antichagasic agents posaconazole-benznidazole based on amorphous solid dispersions. *European Journal of Pharmaceutical Sciences*, *119*, 208–218. <https://doi.org/10.1016/j.ejps.2018.04.024>
- Frank, K. J., Rosenblatt, K. M., Westedt, U., Hölig, P., Rosenberg, J., Mägerlein, M., Fricker, G., & Brandl, M. (2012). Amorphous solid dispersion enhances permeation of poorly soluble ABT-102: True supersaturation vs. apparent solubility enhancement. *International Journal of Pharmaceutics*, *437*(1–2), 288–293. <https://doi.org/10.1016/j.ijpharm.2012.08.014>
- Grohgan, H., Priemel, P. A., Löbmann, K., Nielsen, L. H., Laitinen, R., Mullertz, A., Van den Mooter, G., & Rades, T. (2014). Refining stability and dissolution rate of amorphous drug formulations. *Expert Opinion on Drug Delivery*, *11*(6), 977–989. <https://doi.org/10.1517/17425247.2014.911728>
- Guan, J., Jin, L., Liu, Q., Xu, H., Wu, H., Zhang, X., & Mao, S. (2019). Exploration of supersaturable lacidipine ternary amorphous solid dispersion for enhanced dissolution and in vivo absorption. *European Journal of Pharmaceutical Sciences*. <https://doi.org/10.1016/j.ejps.2019.105043>
- Hate, S. S., Reutzel-Edens, S. M., & Taylor, L. S. (2019). Insight into Amorphous Solid Dispersion Performance by Coupled Dissolution and Membrane Mass Transfer Measurements [Research-article]. *Molecular Pharmaceutics*, *16*(1), 448–461. <https://doi.org/10.1021/acs.molpharmaceut.8b01117>
- Ilevbare, G. A., & Taylor, L. S. (2013). Liquid-liquid phase separation in highly supersaturated aqueous solutions of poorly water-soluble drugs: Implications for solubility enhancing formulations. *Crystal Growth and Design*, *13*(4), 1497–1509. <https://doi.org/10.1021/cg301679h>
- Indulkar, A. S., Gao, Y., Raina, S. A., Zhang, G. G. Z., & Taylor, L. S. (2016). Exploiting the Phenomenon of Liquid-Liquid Phase Separation for Enhanced and Sustained Membrane Transport of a Poorly Water-Soluble Drug. *Molecular Pharmaceutics*, *13*(6), 2059–2069. <https://doi.org/10.1021/acs.molpharmaceut.6b00202>
- Indulkar, A. S., Lou, X., Zhang, G. G. Z., & Taylor, L. S. (2019). Insights into the Dissolution Mechanism of Ritonavir-Copovidone Amorphous Solid Dispersions: Importance of Congruent Release for Enhanced Performance. *Molecular Pharmaceutics*, *16*(3), 1327–1339. <https://doi.org/10.1021/acs.molpharmaceut.8b01261>
- Janssens, S., & Van den Mooter, G. (2009). Review: physical chemistry of solid dispersions. *Journal of Pharmacy and Pharmacology*, *61*(12), 1571–1586. <https://doi.org/10.1211/jpp/61.12.0001>
- Kalepu, S., & Nekkanti, V. (2015). Insoluble drug delivery strategies: Review of recent advances and business prospects. *Acta Pharmaceutica Sinica B*, *5*(5), 442–453. <https://doi.org/10.1016/j.apsb.2015.07.003>
- Kasim, N. A., Whitehouse, M., Ramachandran, C., Bermejo, M., Lennernäs, H., Hussain, A. S., Junginger, H. E., Stavchansky, S. A., Midha, K. K., Shah, V. P., & Amidon, G. L. (2003). Molecular Properties of WHO Essential Drugs and Provisional Biopharmaceutical Classification. *Molecular Pharmaceutics*, *1*(1), 85–96. <https://doi.org/10.1021/MP034006H>
- Krstić, M., Manić, L., Martić, N., Vasiljević, D., Mračević, S. Đ., Vukmirović, S., & Rašković, A. (2020). Binary polymeric amorphous carvedilol solid dispersions: In vitro and in vivo characterization. *European Journal of Pharmaceutical Sciences*, *150*, 105343. <https://doi.org/10.1016/j.ejps.2020.105343>
- Kuo, Y. C., & Chung, J. F. (2011). Physicochemical properties of nevirapine-loaded solid lipid nanoparticles and nanostructured lipid carriers. *Colloids and Surfaces B: Biointerfaces*, *83*(2), 299–306. <https://doi.org/10.1016/j.colsurfb.2010.11.037>

- Lakshman, D., Chegireddy, M., Hanegave, G. K., Sree, K. N., Kumar, N., Lewis, S. A., & Dengale, S. J. (2020a). Investigation of drug-polymer miscibility, biorelevant dissolution, and bioavailability improvement of Dolutegravir-polyvinyl caprolactam-polyvinyl acetate-polyethylene glycol graft copolymer solid dispersions. *European Journal of Pharmaceutical Sciences*, *142*, 105–137. <https://doi.org/10.1016/j.ejps.2019.105137>
- Lakshman, D., Chegireddy, M., Hanegave, G. K., Sree, K. N., Kumar, N., Lewis, S. A., & Dengale, S. J. (2020b). Investigation of drug-polymer miscibility, biorelevant dissolution, and bioavailability improvement of Dolutegravir-polyvinyl caprolactam-polyvinyl acetate-polyethylene glycol graft copolymer solid dispersions. *European Journal of Pharmaceutical Sciences*, *142*, 105–137. <https://doi.org/10.1016/j.ejps.2019.105137>
- Li, N., Mosquera-Giraldo, L. I., Borca, C. H., Ormes, J. D., Lowinger, M., Higgins, J. D., Slipchenko, L. V., & Taylor, L. S. (2016). A Comparison of the Crystallization Inhibition Properties of Bile Salts. *Crystal Growth and Design*, *16*(12), 7286–7300. <https://doi.org/10.1021/acs.cgd.6b01470>
- Li, S., Madan, P., & Lin, S. (2017). Effect of ionization of drug on drug solubilization in SMEDDS prepared using Capmul MCM and caprylic acid. *Asian Journal of Pharmaceutical Sciences*, *12*(1), 73–82. <https://doi.org/10.1016/j.ajps.2016.10.001>
- Lokamatha, K. M., Kumar, S. M. S., & Rao, N. R. (2011). Enhancement of solubility and dissolution rate of nevirapine by solid dispersion technique using dextran: preparation and in vitro evaluation. *International Journal of Pharmaceutical Research & Development*, *2*, 1–8.
- Lopes, C. M., Lobo, J. M. S., Costa, P., Manuel, J., Lobo, S., & Costa, P. (2005). Formas Farmacêuticas de liberação modificada: polímeros hidrofílicos. *Revista Brasileira de Ciências Farmacêuticas*, *41*(2), 143–154.
- Mamatha, T., Naseha, Anitha, N., & Qureshi, H. K. (2017). Development of Nevirapine Tablets by Direct Compression Method Using Solid Dispersion Technique. *Journal of Pharmaceutical Research*, *16*(1), 72. <https://doi.org/10.18579/jpcrck/2017/16/1/112482>
- Meenakshi, & Khan, A. D. (2017). Formulation and Evaluation of Solid Dispersion of Furosemide in Poly vinyl Pyrollidone K 30. *International Journal of ChemTech Research*, *10*(4), 160–171.
- Monschke, M., & Wagner, K. G. (2019). Amorphous solid dispersions of weak bases with pH-dependent soluble polymers to overcome limited bioavailability due to gastric pH variability – An in-vitro approach. *International Journal of Pharmaceutics*, *564*(1), 162–170. <https://doi.org/10.1016/j.ijpharm.2019.04.034>
- Moreton, M. A., Cohen, L., Lepera, L., Bernabeu, E., Taira, C., Höcht, C., & Chiappetta, D. A. (2014). Enhanced oral bioavailability of nevirapine within micellar nanocarriers compared with Viramune®. *Colloids and Surfaces B: Biointerfaces*, *122*, 56–65. <https://doi.org/10.1016/j.colsurfb.2014.06.046>
- Mui, P. W., Jacober, S. P., Hargrave, K. D., & Adams, J. (1992a). Crystal structure of nevirapine, a non-nucleoside inhibitor of HIV-1 reverse transcriptase, and computational alignment with a structurally diverse inhibitor. *Journal of Medicinal Chemistry*, *35*(1), 201–202. <https://doi.org/10.1021/jm00079a029>
- Mui, P. W., Jacober, S. P., Hargrave, K. D., & Adams, J. (1992b). Crystal structure of nevirapine, a non-nucleoside inhibitor of HIV-1 reverse transcriptase, and computational alignment with a structurally diverse inhibitor. *Journal of Medicinal Chemistry*, *35*(1), 201–202. <https://doi.org/10.1021/jm00079a029>
- Pandí, P., Bulusu, R., Kommineni, N., Khan, W., & Singh, M. (2020). Amorphous solid dispersions: An update for preparation, characterization, mechanism on bioavailability, stability, regulatory considerations and marketed products. In *International Journal of Pharmaceutics* (Vol. 586, p. 119560). Elsevier B.V. <https://doi.org/10.1016/j.ijpharm.2020.119560>
- Penzel, E., Rieger, J., & Schneider, H. (1997). The glass transition temperature of random copolymers: 1. Experimental data and the Gordon-Taylor equation. *Polymer*, *38*, 325–327.
- Punčochová, K., Vukosavljević, B., Hanuš, J., Beránek, J., Windbergs, M., & Štěpánek, F. (2016). Non-invasive insight into the release mechanisms of a poorly soluble drug from amorphous solid dispersions by confocal Raman microscopy. *European Journal of Pharmaceutics and Biopharmaceutics*, *101*, 119–125. <https://doi.org/10.1016/j.ejpb.2016.02.001>
- Raina, S. A., Zhang, G. G. Z., Alonzo, D. E., Wu, J., Zhu, D., Catron, N. D., Gao, Y., & Taylor, L. S. (2014). Enhancements and limits in drug membrane transport using supersaturated solutions of poorly water soluble drugs. *Journal of Pharmaceutical Sciences*, *103*(9), 2736–2748. <https://doi.org/10.1002/jps.23826>
- Raju, A., Reddy, A. J., Satheesh, J., & Jithan, A. v. (2014). Preparation and Characterisation of Nevirapine Oral Nanosuspensions. *Indian Journal of Pharmaceutical Sciences*, *76*(1), 62–71. www.ijpsonline.com
- Ranga Rao, K. V., & Devi, K. P. (1988). Swelling controlled release systems: recent development and application. *International Journal of Pharmaceutics*, *48*(1–3), 1–13.
- Saboo, S., Kestur, U. S., Flaherty, D. P., & Taylor, L. S. (2020a). Congruent Release of Drug and Polymer from Amorphous Solid Dispersions: Insights into the Role of Drug-Polymer Hydrogen Bonding, Surface Crystallization, and Glass Transition. *Molecular Pharmaceutics*, *17*(4), 1261–1275. https://doi.org/10.1021/ACS.MOLPHARMACEUT.9B01272/SUPPL_FILE/MP9B01272_SI_001.PDF
- Saboo, S., Kestur, U. S., Flaherty, D. P., & Taylor, L. S. (2020b). Congruent Release of Drug and Polymer from Amorphous Solid Dispersions: Insights into the Role of Drug-Polymer Hydrogen Bonding, Surface Crystallization, and Glass Transition. *Molecular Pharmaceutics*, *17*(4), 1261–1275. https://doi.org/10.1021/ACS.MOLPHARMACEUT.9B01272/SUPPL_FILE/MP9B01272_SI_001.PDF
- Schver, G. C. R. M., & Lee, P. I. (2018). Combined Effects of Supersaturation Rates and Doses on the Kinetic-Solubility Profiles of Amorphous Solid Dispersions Based on Water-Insoluble Poly(2-hydroxyethyl methacrylate) Hydrogels. *Molecular Pharmaceutics*, *15*(5), 2017–2026. <https://doi.org/10.1021/acs.molpharmaceut.8b00162>
- Sevam, R. P., & Kulkarni, P. K. (2014). Design and Evaluation of Self Nanoemulsifying Systems for Poorly Water Soluble HIV. *Journal of PharmaSciTech*, *4*(1), 23–28.
- Shegokar, R., & Singh, K. K. (2011). Surface modified nevirapine nanosuspensions for viral reservoir targeting: In vitro and in vivo evaluation. *International Journal of Pharmaceutics*, *421*(2), 341–352. <https://doi.org/10.1016/j.ijpharm.2011.09.041>

- Shi, Q., Chen, H., Wang, Y., Wang, R., Xu, J., & Zhang, C. (2022). Amorphous Solid Dispersions: Role of the Polymer and Its Importance in Physical Stability and In Vitro Performance. *Pharmaceutics*, *14*(8). <https://doi.org/10.3390/pharmaceutics14081747>
- Shi, Q., Chen, H., Wang, Y., Wang, R., Xu, J., Zhang, C., Shi, Q., Chen, H., Wang, Y., Wang, R., Xu, J., & Zhang, C. (2022). Amorphous Solid Dispersions: Role of the Polymer and Its Importance in Physical Stability and In Vitro Performance. *Pharmaceutics* 2022, Vol. 14, Page 1747, *14*(8), 1747. <https://doi.org/10.3390/PHARMACEUTICS14081747>
- Sun, D. D., & Lee, P. I. (2013). Evolution of supersaturation of amorphous pharmaceuticals: The effect of rate of supersaturation generation. *Molecular Pharmaceutics*, *10*(11), 4330–4346. <https://doi.org/10.1021/mp400439q>
- Sun, D. D., & Lee, P. I. (2015a). Probing the mechanisms of drug release from amorphous solid dispersions in medium-soluble and medium-insoluble carriers. *Journal of Controlled Release*, *211*, 85–93. <https://doi.org/10.1016/j.jconrel.2015.06.004>
- Sun, D. D., & Lee, P. I. (2015b). Evolution of supersaturation of amorphous pharmaceuticals: Nonlinear rate of supersaturation generation regulated by matrix diffusion. *Molecular Pharmaceutics*, *12*(4), 1203–1215. <https://doi.org/10.1021/mp500711c>
- Sun, D. D., & Lee, P. I. (2015c). Haste Makes Waste: The Interplay Between Dissolution and Precipitation of Supersaturating Formulations. *AAPS Journal*, *17*(6), 1317–1326. <https://doi.org/10.1208/s12248-015-9825-6>
- Tambosi, G., Coelho, P. F., Soares, L., Lenschow, I. C. S., Zétola, M., Stulzer, H. K., & Pezzini, B. R. (2018). Challenges to improve the biopharmaceutical properties of poorly water-soluble drugs and the application of the solid dispersion technology. *Revista Materia*, *23*(4). <https://doi.org/10.1590/s1517-707620180004.0558>
- Trasi, N. S., & Taylor, L. S. (2015). Thermodynamics of Highly Supersaturated Aqueous Solutions of Poorly Water-Soluble Drugs—Impact of a Second Drug on the Solution Phase Behavior and Implications for Combination Products. *Journal of Pharmaceutical Sciences*, *104*(8), 2583–2593.
- Varshosaz, J., Taymouri, S., Jafari, E., Jahanian-Najafabadi, A., & Taheri, A. (2018). Formulation and characterization of cellulose acetate butyrate nanoparticles loaded with nevirapine for HIV treatment. *Journal of Drug Delivery Science and Technology*. <https://doi.org/10.1016/j.jddst.2018.08.020>
- Wypych, G. (2012). PVP poly(N-vinyl pyrrolidone). In *Handbook of Polymers* (pp. 628–630). Elsevier. <https://doi.org/10.1016/B978-1-895198-47-8.50185-5>
- Zhang, X., Xing, H., Zhao, Y., & Ma, Z. (2018). Pharmaceutical dispersion techniques for dissolution and bioavailability enhancement of poorly water-soluble drugs. *Pharmaceutics*, *10*(3). <https://doi.org/10.3390/pharmaceutics10030074>